Materials Science and Engineering A 486 (2008) 49–55

MATERIALS SCIENCE & ENGINEERING A

www.elsevier.com/locate/msea

Effect of microstructural evolution on mechanical properties of friction stir welded ZK60 alloy

G.M. Xie [a,b], Z.Y. Ma [a,*], L. Geng [b]

[a] *Institute of Metal Research, Chinese Academy of Sciences, 72 Wenhua Road, Shenyang 110016, China*

[b] *School of Materials Science and Engineering, Harbin Institute of Technology, Harbin 150001, China*

Received 5 June 2007; received in revised form 18 August 2007; accepted 21 August 2007

Abstract

Six millimeters thick extruded ZK60 plate was successfully friction stir welded at a rotation rate of 800 rpm and a traverse speed of 100 mm/min. Friction stir welding (FSW) resulted in breakup and dissolution of $MgZn_2$ phase and remarkable grain refinement in the nugget zone. Relatively weak basal texture on the transverse plane of the nugget zone was not the dominant factor for determining the mechanical properties of the ZK60 weld. As-welded joints failed on the nugget zone with ultimate tensile strength (UTS) reaching 87% of the parent material. After aging, the precipitation of the fine $MgZn_2$ particles increased the mechanical properties of the weld significantly with the UTS reaching 94% of the parent material and the fracture occurring in the heat-affected zone. The fracture locations under both as-welded and aged conditions were consistent with the lowest hardness distribution of the welds.

Keywords: Friction stir welding; Magnesium alloy; Aging; Texture; Hardness; Strength

1. Introduction

Magnesium alloys have drawn a great deal of attention from automotive and aerospace industries, where weight saving are of great importance, due to their low density, high specific strength and high specific rigidity and good damping capacity [1,2]. Currently, magnesium alloy parts are mainly produced by casting, and the use of other manufacture technologies, such as plastic forming and welding, is still limited [3–5]. It is necessary to develop effective and inexpensive welding techniques for industrial applications of magnesium alloys. Friction stir welding (FSW) is a relatively new solid-state joining technique, invented by The Welding Institute of the UK in 1991 [6]. It has been indicated that FSW is an effective technique for joining aluminum, magnesium, copper, titanium, steel, and metal matrix composites [7].

In the past few years, research on FSW of magnesium alloys, including AZ (Mg–Al–Zn), AM (Mg–Al–Mn), heat-resistant magnesium alloys (Mg–Al–Ca and Mg–Zn–Y–Zr) has been reported [8–17]. From the investigations on these magnesium alloys it was seen that sound FSW joints with good properties and uniform microstructure can be achieved under optimized FSW parameters. While Nakata et al. [8] and Lee et al. [9] reported that sound joints were produced only at higher tool rotation rates and lower traverse speeds in thixomolded AZ91D and hot-rolled AZ31B-H24, the investigations by Lee et al. [10] and Park et al. [11] indicated that defect-free FSW welds of AZ91D could be achieved at relatively high tool rotation rates of 800–1600 rpm for a wide range of tool traverse speeds. Similarly, Esparza et al. [12] reported that under a higher rotation rate of 2000 rpm and a lower traverse speed of 120 mm/min, 2 mm thick thixomolded AM60 plates were welded via FSW without any defect. Recently, sound friction stir welds in 2 mm thick thixomolded Mg–Al–Ca plate and 6 mm thick forged Mg–Zn–Y–Zr plate were successfully produced by Zhang et al. [15] and Xie et al. [16] under relatively low heat inputs (1500 rpm–1500 mm/min and 800 rpm–100 mm/min, respectively).

To the best of our knowledge, no attempt has been made so far to evaluate the weldability of ZK (Mg–Zn–Zr) alloys via FSW. Because the fine Mg–Zn particles are the main strengthening phase in Mg–Zn–Zr alloy, the microstructural evolution

* Corresponding author. Tel.: +86 24 83978908; fax: +86 24 83978908.
E-mail address: zyma@imr.ac.cn (Z.Y. Ma).

0921-5093/$ – see front matter © 2007 Elsevier B.V. All rights reserved.
doi:10.1016/j.msea.2007.08.043

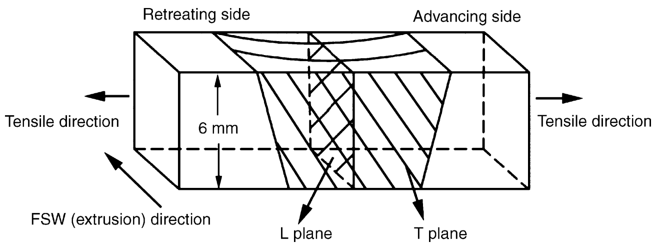

Fig. 1. Schematic illustration of the L and T planes in the nugget zone.

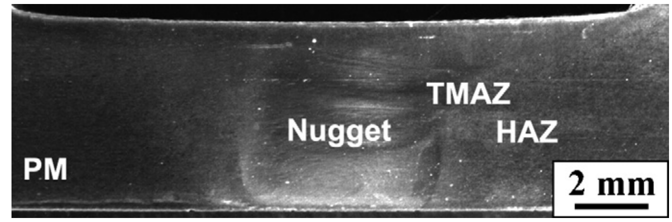

Fig. 2. Cross-sectional macrograph of FSW ZK60 magnesium alloy weld (the advancing side is on the right).

during FSW and mechanical response of FSW Mg–Zn–Zr joint might be quite different from other FSW magnesium alloys reported before. In this study, we reported the first result on FSW of Mg–Zn–Zr alloy and discussed the correlation between microstructure and hardness profile/fracture location of the FSW joints in the different magnesium alloy systems.

2. Experimental procedure

ZK60 alloy extrusion plates of 8 mm in thickness and 100 mm in width with a composition of 6.0Zn–0.6Zr (in wt.%) were used for this study. Six millimeters thick plates were machined from the extrusions and welded along the extrusion direction at a tool rotation rate of 800 rpm and a traverse speed of 100 mm/min by using a gantry FSW machine (China FSW Center). A tool with a shoulder of 20 mm in diameter and a coniform threaded pin of 6 mm in diameter and 5.7 mm in length was used. The tilt angle for all welds was maintained at 2.5°. Before welding, the plates were cleared by the wire brush to remove the surface oxide layer. After FSW, part of the FSW samples were subjected to artificial aging (T5, 150 °C/24 h). The FSW samples were cross-sectioned perpendicular to the welding direction, polished and then etched with solution of 90 ml ethanol, 10 ml distilled water, 5 ml acetic acid and 5 g picric acid. Microstructural features were characterized by optical microscopy (OM) and scanning electron microscopy (SEM). Grain sizes were measured by the mean linear intercept method. Phase composition of the nugget zone and texture of the nugget zone and parent material (PM) were analyzed by Philips type X-ray diffractometer (XRD) with Cu Kα radiation. The specimens for texture measurement were obtained on the transverse cross-sectional plane (T plane) and longitudinal plane (L plane) of the nugget zone of the weld as illustrated in Fig. 1. Similarly, the texture measurements on the PM were also conducted on the welded butt surface of the PM (L plane) and T plane which is perpendicular to the extrusion direction. The Vickers hardness of the joint was measured with a 500 g load for 13 s by LECO-LM247AT type Vickers-hardness machine. The tensile specimens with a gauge length of 40 mm and a gauge width of 10 mm were machined perpendicular to the FSW direction. The tensile test was carried out using the Zwick–Roell type testing machine at a strain rate of $4.2 \times 10^{-4}\ \mathrm{s}^{-1}$.

3. Results and discussion

A cross-sectional macrograph of FSW ZK60 joint is presented in Fig. 2. No welding defect was detected in the joint, indicating that the sound FSW ZK60 joint can be achieved under investigated welding parameter (rotation rate of 800 rpm and traverse speed of 100 mm/min). Three microstructural zones were identified in the FSW ZK60 joint, i.e. the nugget zone, thermomechanically affected zone (TMAZ) and heat-affected zone (HAZ). Fig. 3 shows the microstructures of the parent material, TMAZ and nugget zone. The parent material exhibited the coarse deformed structures with a large number of unordered flow lines and some precipitates being distributed between coarse grains (Fig. 3(a)). In the TMAZ, the elongated grains distributed along flow line were observed, and it appears that the dynamic recrystallization did not occur due to insufficient deformation strain and thermal exposure (Fig. 3(b)). The microstructure of the nugget zone was characterized by the fine and equiaxed grains of 5.3 μm, indicating the occurrence of dynamic recrystallization due to intense plastic deformation and thermal exposure during FSW (Fig. 3(c)). Esparza et al. [12] and Park et al. [13] reported the generation of the recrystallized grains of 10–15 μm in the nugget zone of FSW AM60 and AZ61 alloys. Clearly, the grain size obtained in the FSW ZK60 alloy is much smaller than that in the FSW AM60 and AZ61 alloys. This is attributed to obvious grain refinement effect resulting from zirconium element. Beyond the TMAZ there is a HAZ, which experiences a thermal cycle without any plastic deformation.

Under temperature of FSW, both basal and non-basal slip systems should operate. However, at relatively high strain of FSW, only limited non-basal slip systems would operate, i.e. basal plane slip is the main deformation mechanism [18,19]. The XRD patterns of the PM and nugget zone, used for analysis of texture, are shown in Fig. 4. Based on XRD results, the relative intensity of diffraction peak was defined:

$$I_{\text{relative}} = \frac{[I_{(h\,k\,i\,l)}/(I_{(1\,0\,\bar{1}\,0)} + I_{(0\,0\,0\,2)} + I_{(1\,0\,\bar{1}\,1)} + I_{(1\,1\,\bar{2}\,0)})]_{\text{sample}}}{[I_{(h\,k\,i\,l)}/(I_{(1\,0\,\bar{1}\,0)} + I_{(0\,0\,0\,2)} + I_{(1\,0\,\bar{1}\,1)} + I_{(1\,1\,\bar{2}\,0)})]_{\text{random-Mg-powder}}} \qquad (1)$$

where $(0\,0\,0\,2)$ is a basal plane, both $(1\,0\,\bar{1}\,0)$ and $(1\,1\,\bar{2}\,0)$ are the cylindrical faces perpendicular to $(0\,0\,0\,2)$ plane, and the intensity of random Mg powder came from standard PDF card. The relative intensities of calculated XRD at various planes are listed in Table 1. Depended on the relative intensity, the preferred orientation at each plane (L and T planes) can be roughly confirmed. As seen from the L plane of the PM specimen, the $(0\,0\,0\,2)$ plane exhibited a higher relative intensity of ∼4.63, whereas $(1\,0\,\bar{1}\,0)$

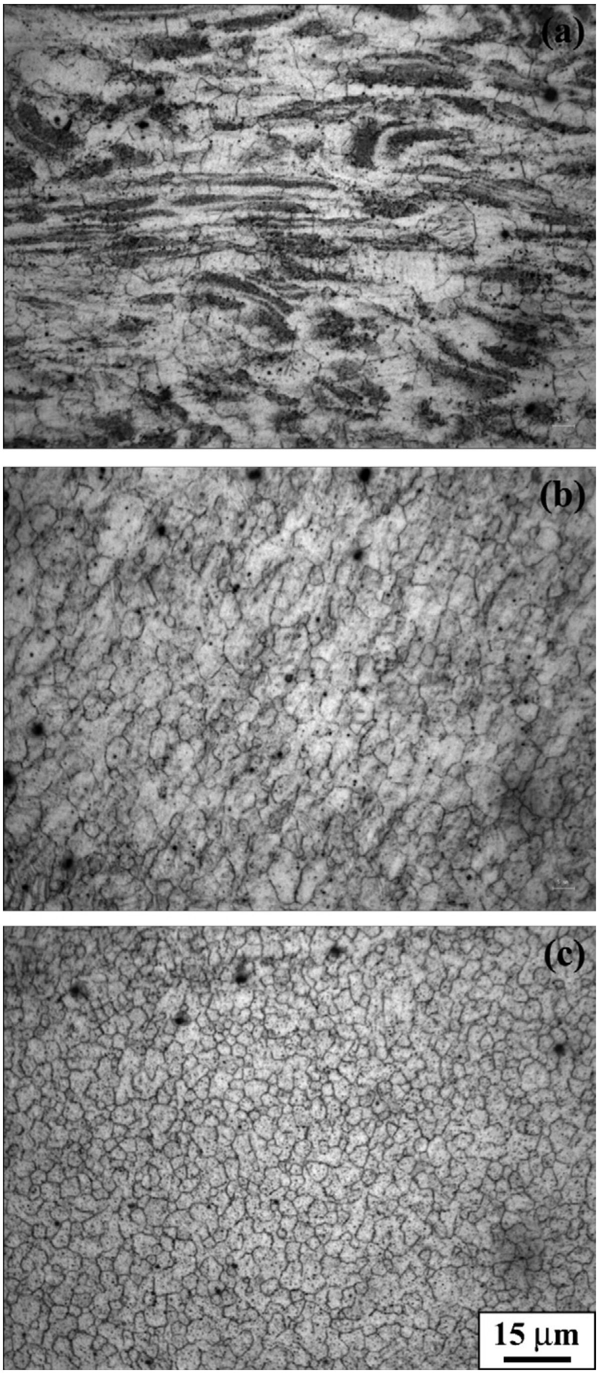

Fig. 3. Microstructure of FSW ZK60 joint: (a) PM, (b) TMAZ, and (c) nugget zone.

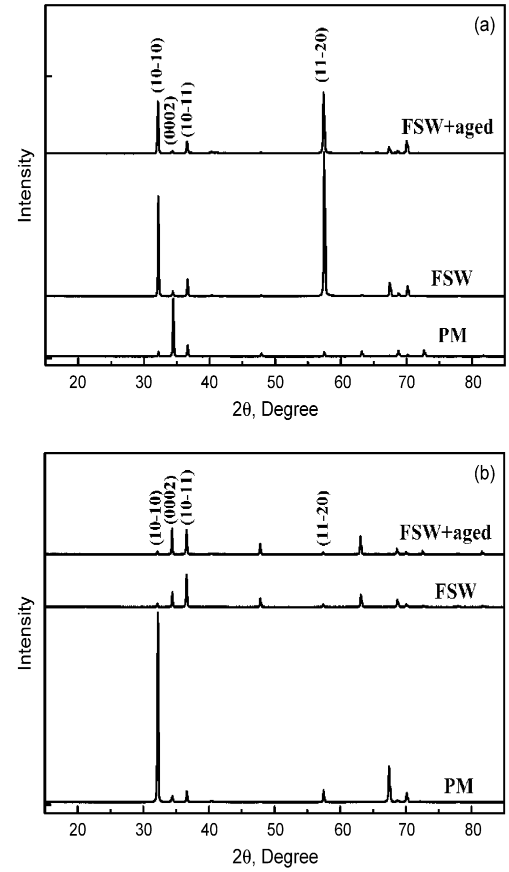

Fig. 4. XRD patterns obtained from (a) L plane and (b) T plane.

Table 1
Relative XRD intensity measured from the T and L planes of the FSW joints and as-extruded PM

Material	L plane			T plane		
	$(0\,0\,0\,2)$	$(1\,0\,\bar{1}\,0)$	$(1\,1\,\bar{2}\,0)$	$(0\,0\,0\,2)$	$(1\,0\,\bar{1}\,0)$	$(1\,1\,\bar{2}\,0)$
PM	4.63	0.39	0.68	0.18	5.74	0.67
FSW	0.11	2.50	6.51	1.70	0.46	0.61
FSW + aged	0.12	2.69	5.82	2.90	0.38	0.45

and $(1\,1\,\bar{2}\,0)$ planes showed a lower relative intensity of ~0.39 and ~0.68, respectively. In the T plane, while the $(1\,0\,\bar{1}\,0)$ plane had a stronger relative intensity of ~5.74, the $(0\,0\,0\,2)$ plane had a lower intensity of ~0.18. Thus, most of basal plane $(0\,0\,0\,2)$ was parallel to the L plane, and amount of $(1\,0\,\bar{1}\,0)$ plane on the T plane was predominant. Because the $(0\,0\,0\,2)$ basal plane on the extrusion flat plane (L plane) is typical for the hexagonal Mg alloys [20], the PM of ZK60 on the L and T planes has strong basal texture. After FSW, the relative intensity of $(0\,0\,0\,2)$, $(1\,0\,\bar{1}\,0)$ and $(1\,1\,\bar{2}\,0)$ planes are ~0.11, ~2.5 and ~6.5 on the L plane, and ~1.70, ~0.46 and ~0.61 on the T plane, respectively (Table 1). Based on above observations, it is suggested that FSW transformed the grain preferred orientation from $(0\,0\,0\,2)$ of the PM to $(1\,0\,\bar{1}\,0)$ and $(1\,1\,\bar{2}\,0)$ of the nugget zone on the L plane (Fig. 4(a)), simultaneously, the $(1\,0\,\bar{1}\,0)$ plane preferred orientation was changed to $(0\,0\,0\,2)$ plane on the T plane after FSW (Fig. 4(b)). Difference of relative intensity between $(0\,0\,0\,2)$ and $(1\,0\,\bar{1}\,0)/(1\,1\,\bar{2}\,0)$ planes on the T plane of the nugget zone is small, whereas the relative intensity of $(1\,0\,\bar{1}\,0)$ and $(1\,1\,\bar{2}\,0)$ planes was much higher than that of $(0\,0\,0\,2)$ plane on the L plane. Clearly, most of $(1\,0\,\bar{1}\,0)$ and $(1\,1\,\bar{2}\,0)$ planes lay on the L plane, thus, the strong orientation appeared at the center location of the weld (T plane). On the T plane of the nugget zone, part of $(0\,0\,0\,2)$ basal plane was parallel to the T plane, therefore, the T plane exhibited a weak basal texture.

Recently, Park et al. [19] studied the microtexture of AZ61 alloy in detail and they suggested that an intense $(0\,0\,0\,2)$ basal

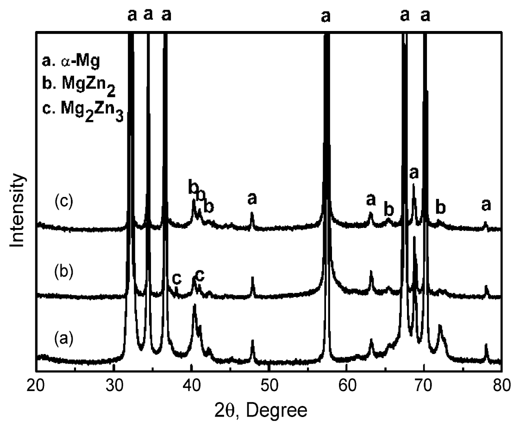

Fig. 5. XRD patterns of ZK60 magnesium alloy: (a) PM, (b) as-welded nugget zone, and (c) aged nugget zone.

plane texture, whose trace became an ellipsolid and which roughly surrounded the pin column surface of the welding tool, was produced in most parts of the nugget zone. More recently, Wang et al. [21] reported that the Schmid factor (0.3) of the nugget zone was higher than that of the extruded AZ31 sample (∼0), i.e. the texture of the nugget zone on the transverse plane of the weld was weaker than that of the extruded PM. Therefore, from the texture distribution, it is seen that the texture in the nugget zone of FSW ZK60 in this study is consistent with that of FSW AZ61, i.e. average texture on the T plane of the weld is weaker than that of the PM. Furthermore, the texture of the aged nugget zone was similar to that of the as-welded nugget zone for this ZK60 alloy (Table 1).

Fig. 5 shows the XRD patterns of the nugget zone under as-welded and aged conditions. For the PM and the nugget zones under two conditions, the diffraction peaks of α-Mg and $MgZn_2$ were detected. Furthermore, in the nugget zone of the as-welded joint the diffraction peaks of Mg_2Zn_3 were also found. Sturkey and Clark [22] pointed out that the β′ phase, which is similar to the laves phase ($MgZn_2$) in structure, is main precipitate in Mg–Zn alloys. During the hot extrusion, most of precipitates were dissolved into the magnesium matrix. Therefore, only a small amount of precipitates with a size of up to 4 μm were observed in the as-extruded PM (Fig. 6(a)). FSW resulted in the breakup and further dissolution of the precipitates due to thermal exposure and intense plastic deformation. Thus, the amount and size of the precipitates in the nugget zone were significantly reduced (Fig. 6(b)). Clearly, under both as-extruded and as-welded conditions, fast cooling from extrusion and FSW temperatures retained most of Zn in solution. In this case, it is expected that the T5-treatment will exert a significant influence on the microstructure of both the PM and nugget zone. Compared to that in the as-extruded PM (Fig. 6(a)), the amount

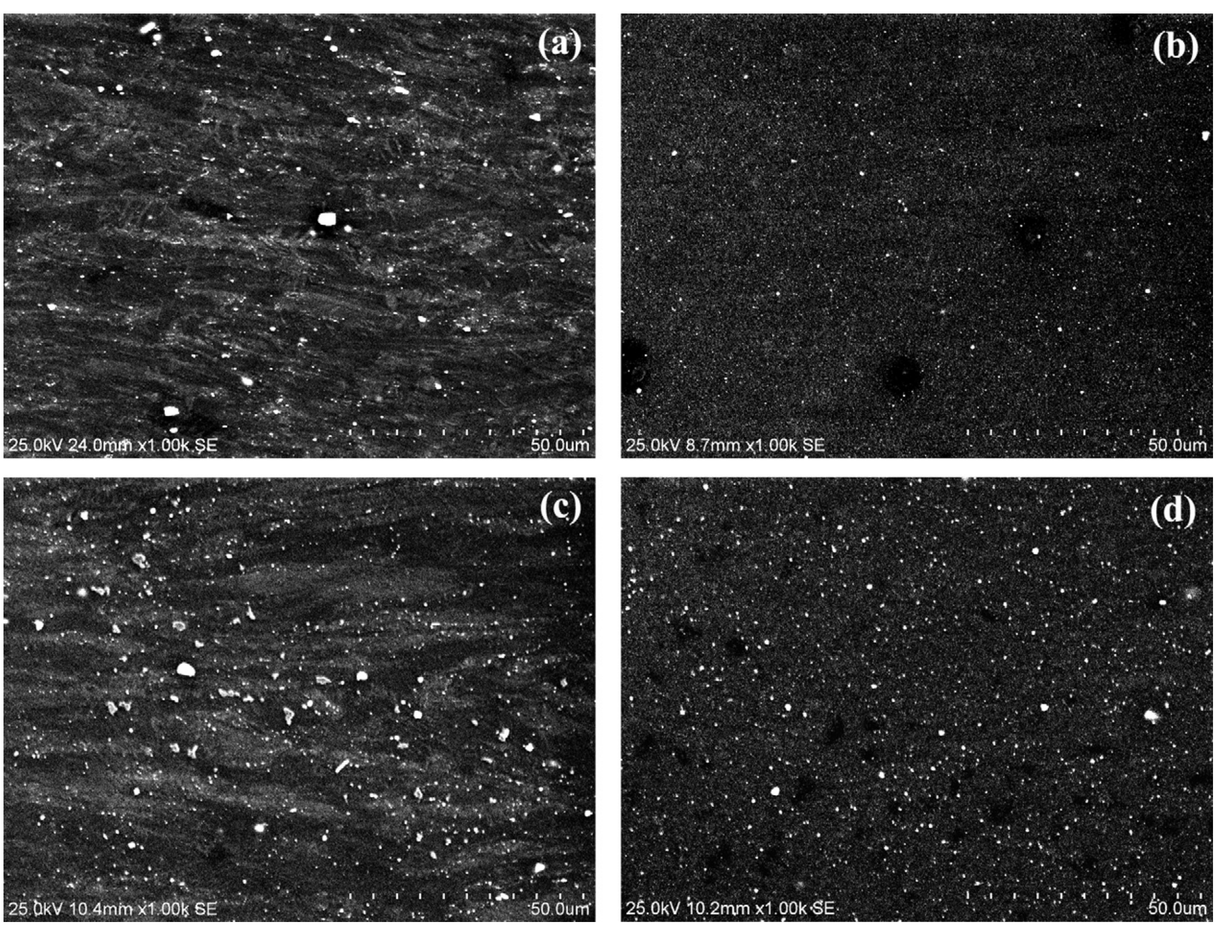

Fig. 6. SEM images of ZK60 magnesium alloy: (a) as-extruded PM, (b) as-welded nugget zone, (c) aged PM, and (d) aged nugget zone.

of the precipitates in the T5-treated PM increased significantly (Fig. 6(c)). However, the size of the largest precipitates was similar in both samples. For the nugget zone, the T5-treatment resulted in the generation of fine and homogeneously distributed precipitates. Compared to the T5-treated PM, the size of the precipitates in the T5-treated nugget zone was much finer and the distribution uniformity of the precipitates was significantly improved.

Recently, Zhang et al. [15] and Xie et al. [16] reported that during FSW of Mg–Al–Ca and Mg–Zn–Y–Zr magnesium alloys, bulky intermetallic compounds (Al_2Ca and Mg–Zn–Y phases) were broken up and dispersed in the nugget zone, resulting in remarkable increase in hardness values. Therefore, in their hardness curves [15,16], the hardness values in the nugget zone were substantially higher than those of other zones. On the other hand, Park et al. [13] and Chang et al. [14] reported that the hardness values of FSW wrought and extruded AZ61 throughout various zones of the weld were uniform. Similarly, Esparza et al. [12] also found that FSW AM60 weld exhibited similar hardness values across the whole weld. It was suggested that coarse eutectic β-$Al_{12}Mg_{17}$ phase hardly contributed to the average hardness value of the PM [23], therefore, the dissolution of β-$Al_{12}Mg_{17}$ phase in the nugget zone during FSW did not result in the noticeable change of hardness across the weld zone for AZ and AM system magnesium alloys. ZK60 is a precipitation-strengthening magnesium alloy, and the $MgZn_2$ precipitates in ZK60 magnesium alloy are much finer than $Al_{12}Mg_{17}$ particles in AZ and AM system alloys. Therefore, the hardness of the ZK60 alloy is mainly governed by the precipitates. Fig. 7 shows the hardness profile along the centerline on the cross-section of the FSW ZK60 joint under both as-welded and aged conditions. The hardness values within the nugget zone of the as-welded joint were significantly lower than those of the PM and other zones due to the further dissolution of $MgZn_2$ particles during FSW (Fig. 6(b)). In this case, the precipitate rather than the grain size is the dominant factor to govern the hardness of the nugget zone. The hardness profile observed in this FSW ZK60 alloy is quite different from that in other FSW magnesium alloys [12–16]. After aging, the hardness values in both PM and weld were significantly increased due to the precipitation-hardening. However, the hardness values of the nugget zone were obviously higher than those of the PM. This is attributed to significantly refined and uniformly distributed $MgZn_2$ precipitates and remarkably refined grains (Figs. 3(c) and 6(d)).

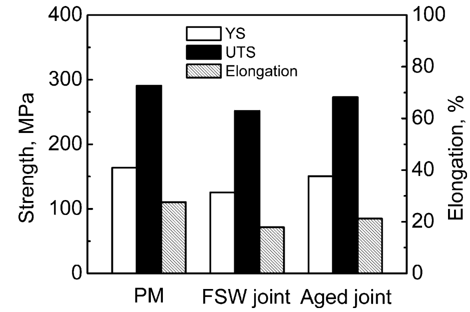

Fig. 8. Transverse tensile properties of FSW ZK60 magnesium alloy.

Furthermore, it is noted that there was a the lowest-hardness zone in the HAZ of the T5-treated weld on the advancing side. This is attributed to coarsened grain structure in this zone.

Xie et al. noted that for the FSW heat-resistant Mg–Zn–Y–Zr alloy, the fracture of transverse tensile specimens occurred at the HAZ because the hardness of the HAZ was much lower than that of the nugget zone [16]. Therefore, Mg–Zn–Y ternary phase with high hardness value exerted a significant effect on the mechanical properties of the FSW joint. Park et al. [13] reported that under a relative uniform hardness profile, the fracture of transverse tensile specimens of the FSW AZ61 joint occurred at the nugget zone. As discussed above, eutectic β-$Al_{12}Mg_{17}$ phase in the AZ system magnesium alloys hardly affected the hardness profile, therefore, the texture is the dominant factor for determining the mechanical properties of the FSW AZ61 joint. Because the basal planes of the nugget zone surrounded the pin column, thus, the maximum resolved shear stress operated on (0 0 0 2) plane, which is a 45° angle with the tensile direction [13]. Compared to the coarse β-$Al_{12}Mg_{17}$ phase in the AZ system alloys, the fine $MgZn_2$ particles in the ZK60 alloy exerted a significant strengthening effect on the magnesium matrix, therefore, the effect of precipitation strengthening on the mechanical properties is dominant for ZK60 alloy. The transverse tensile properties of the FSW ZK60 joint are shown in Fig. 8. Compared to the PM, the as-FSW joint exhibited decreased ultimate tensile and yield strengths (UTS and YS) and elongation-to-failure (El.) that were 87%, 77%, and 67% of the PM, respectively, with the fracture occurring in the nugget zone (Fig. 9(a)) and the fracture surface being characterized by the large dimples and tearing edges (Fig. 10(a)), indicating the occurrence of significant plastic deformation in the nugget zone. In this case, the transverse UTS and YS of the weld are those of the nugget zone, i.e. the

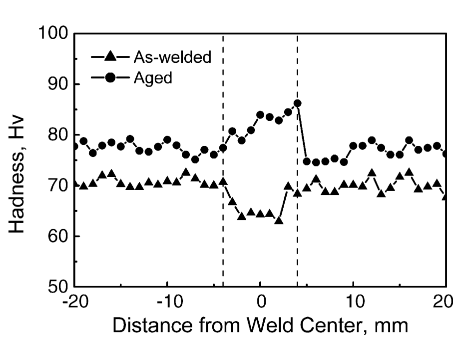

Fig. 7. Hardness profile of FSW ZK60 magnesium alloy joint.

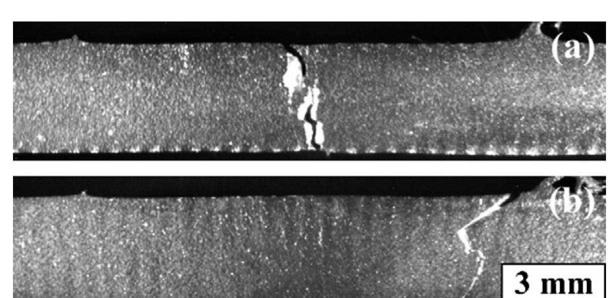

Fig. 9. Failed FSW ZK60 joints under (a) as-welded and (b) aged conditions.

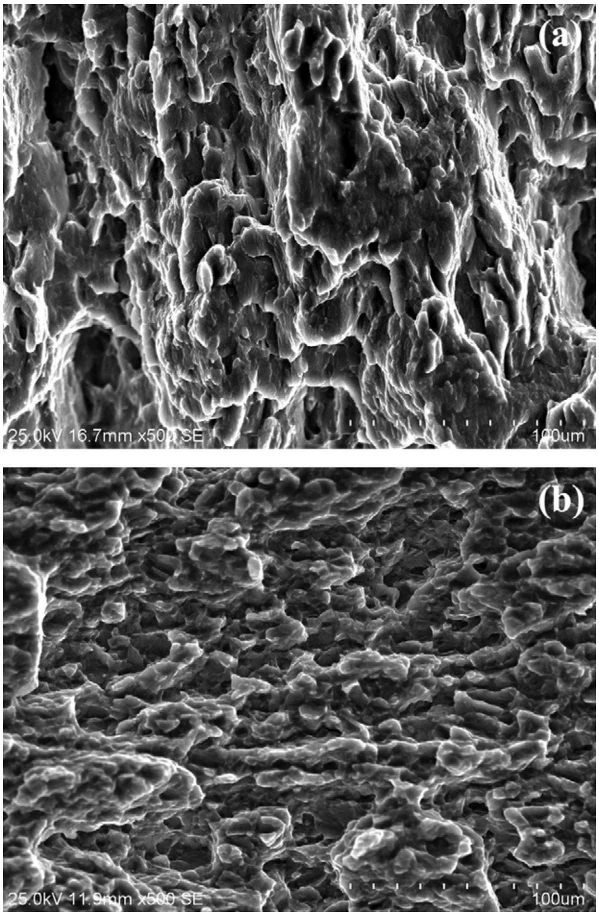

Fig. 10. SEM images showing fracture surfaces of FSW ZK60 joint under (a) as-welded and (b) aged conditions.

weakest zone in the whole weld due to significant dissolution of the $MnZn_2$ phase (Fig. 6(b)). In contrast to the as-welded joint, aged joint exhibited increased UTS, YS and ductility that reached 94%, 92%, and 77% of the PM, respectively, with the fracture occurring in the HAZ on the advancing side (Fig. 9(b)) and the fracture surface being characterized by the fine dimples (Fig. 10(b)), indicating the increased strength. Because the texture distributions of the welds under both as-welded and aged conditions were similar (Table 1 and Fig. 4), therefore, the tensile properties and fracture characteristics of the welds were primarily governed by the precipitates. The change of the fracture location under different conditions was consistent with that of the lowest hardness distribution in the nugget zone (Fig. 7). For the aged weld, the HAZ is the weakest zone in the whole weld. Therefore, the transverse tensile and yield strengths of the aged weld are lower than those of the PM, though obvious aging strengthening was observed in the nugget zone of the aged sample.

Recently, Lee et al. [10] and Chang et al. [14] reported that the UTS of FSW hot-rolled AZ31B-H24 and extruded AZ61C-F joints were 85% and 70% of the PM, respectively. In this study, the UTS of the aged FSW ZK60 joint reached 94% of the PM. The joining efficiency (UTS_{FSW}/UTS_{PM}) achieved for ZK60 alloy exceeded that for AZ31B-H24 and AZ61C-F alloys and was similar to that for Mg–Zn–Y–Zr [16].

4. Conclusions

1. Under a rotation rate of 800 rpm and a traverse speed of 100 mm/min, 6 mm thick extruded ZK60 magnesium alloy plate was successfully friction stir welded and defect-free weld was obtained.
2. The transverse plane (T plane) of the nugget zone exhibited the relative weaker basal texture compared to the PM, and basal planes were around the pin.
3. During FSW, fine and equiaxed recrystallized grains of 5.3 μm were generated and $MgZn_2$ particles were broken up and dispersed with most of them being dissolved into the magnesium matrix. Post-weld aging resulted in precipitation of fine and uniformly distributed $MgZn_2$ particles.
4. The UTS, YS and elongation of the FSW joint reached 87%, 77%, and 65% of the PM, respectively. After aging treatment, UTS, YS and elongation were increased to 94%, 92%, and 77% of the PM, respectively.
5. The fracture of the FSW joints occurred at the nugget zone and HAZ under as-welded and aged conditions, respectively, which was consistent with the lowest hardness distribution of the welds.

Acknowledgements

This work was supported by the National Outstanding Young Scientist Foundation for Z.Y. Ma under Grant No. 50525103, the National Basic Research Program of China under Grant No. 2006CB605205, and the Hundred Talents Program of Chinese Academy of Sciences.

References

[1] I.J. Polmear, Light Alloys, 3rd ed., Arnold, London, 1995.
[2] M.M. Avedesian, H. Baker (Eds.), Magnesium and Magnesium Alloys, ASM, USA, 1999.
[3] A. Styczynski, Ch. Hatig, J. Bohlen, D. Letzig, Scripta Mater. 50 (2004) 943.
[4] J. Koike, T. Kobayashi, T. Mukai, H. Watanabe, M. Suzuki, K. Maruyama, K. Higashi, Acta Mater. 51 (2003) 2055.
[5] A. Munitz, C. Colter, A. Stern, G. Kohn, Mater. Sci. Eng. A 302 (2001) 68.
[6] W.M. Thomas, E.D. Nicholas, J.C. Needham, M.G. Murch, P. Templesmith, C.J. Dawes, GB Patent Application No. 9125978.8 (December 1991).
[7] R.S. Mishra, Z.Y. Ma, Mater. Sci. Eng. R 50 (2005) 1.
[8] K. Nakata, S. Inoki, Y. Nagano, T. Hashimoto, S. Johgan, M. Ushio, Proceedings of the third International Symposium on Friction Stir Welding, Kobe, Japan, September 27–28, 2001.
[9] W.B. Lee, J.W. Kim, Y.M. Yeon, S.B. Jung, Mater. Trans. 44 (2003) 917.
[10] W.B. Lee, Y.M. Yeon, S.B. Jung, Mater. Sci. Technol. 19 (2003) 785.
[11] S.H.C. Park, Y.S. Sato, H. Kokawa, J. Mater. Sci. 38 (2003) 4379.
[12] J.A. Esparza, W.C. Davis, L.E. Murr, J. Mater. Sci. 38 (2003) 941.
[13] S.H.C. Park, Y.S. Sato, H. Kokawa, Scripta Mater. 49 (2003) 161.
[14] W.S. Chang, H.J. Kim, J.S. Noh, H.S. Bang, Key Eng. Mater. 321–323 (2006) 1723.
[15] D. Zhang, M. Suzuki, K. Maruyama, Scripta Mater. 52 (2005) 899.
[16] G.M. Xie, Z.Y. Ma, L. Geng, R.S. Chen, Mater. Sci. A 471 (2007) 63.

[17] M.A. Gharacheh, A.H. Kokabi, G.H. Daneshi, B. Shalchi, R. Sarrafi, Int. J. Mach. Tool Manuf. 46 (2006) 1983.
[18] C.I. Chang, C.J. Lee, J.C. Huang, Scripta Mater. 51 (2004) 509.
[19] S.H.C. Park, Y.S. Sato, H. Kokawa, Metall. Mater. Trans. 34A (2003) 987.
[20] Y.N. Wang, J.C. Huang, Mater. Chem. Phys. 81 (2003) 11.
[21] Y.N. Wang, C.I. Chang, C.J. Lee, H.K. Lin, J.C. Huang, Scripta Mater. 55 (2006) 637.
[22] L. Sturkey, J.B. Clark, J. Inst. Met. 88 (1959–1960) 177.
[23] K. Ishikawa, Y. Kobayashi, T. Shibusawa, J. Jpn. Inst. Met. 61 (1997) 1031.